Effect of Sputtering Technique and Properties of TiO_2 Doped with SnO_2 Thin Films

Manjula N[1], Selvan G[1,3], Ayeshamariam A[1,2,4*], Mohamed Saleem A[2,5], Geetha N[1,6] and Jayachandran M[7]

[1]Research and Development Center, Bharathiyar University, Coimbatore, 641076, India
[2]Research and Development Center, Bharathidasan University, Tiruchirappalli, 620024, India
[3]Department of Physics, Thanthai Hans Roever College, Perambalur, India
[4]Department of Physics, Khadir Mohideen College, Adirampattinam, 614 701, India
[5]Department of Physics, Jamal Mohamed College (Auto), Thiruchirappalli, 620 020, India
[6]Department of Physics, Kunthavai Nachiyar Government Arts College for Women, Thanjavur, 613 007, India
[7]Department of Physics, Sethu Institute of Technology, Pullor, Kariapatti, 626 106, India

Abstract

Doped oxide materials of 90% of TiO_2 was doped with 10% of SnO_2 that target has been deposited at a substrate temperature of 250°C for 1 hour by using DC Sputtering technique. The as synthesized target was TiO_2-SnO_2 was used to deposit on the glass substrates. The deposited oxide thin film was characterized for their structural, surface morphological, electrical and optical properties. X-ray diffraction is used for studying the nature and structure, scanning electron, atomic force microscopy and transmission electron microscopy are used to identify the surface morphology of the prepared films. The Van der Pauw technique is employed to measure electrical resistivity and Hall mobility of the film. Wide varieties of methods are available for measuring thin film thicknesses. Stylus profilometry will be helpful to find the thickness of the film, structural studies by X-ray, and micros structural analysis of the film.

Keywords: TiO_2-SnO_2; Stylus profilometry; X-ray diffraction (XRD); UV-Vis-NIR spectrometer; Scanning Electron microscopy (SEM)

Introduction

The TiO_2 nano-particles are area of interest due to their unique technological properties and applications for dye-sensitized solar cell (DSSC). We reported the applications of the TiO_2 thin film based different doped materials. The nanostructures TiO_2 exists in three polymorphic phase viz. rutile, anatase and brookite, SnO_2 is one of the candidates for electrodes due to its rich resources, low cost, good capacitance performance, and the agglomeration of SnO_2 efficiently by anchoring SnO_2 particles onto its interlamellar surfaces. Finding good electrode materials is the key to the development of super capacitor systems; SnO_2 is one of the candidates for electrodes due to its rich resources, low cost, good capacitance performance, showing potential applications in energy storage devices. ZnO-SnO_2 heterostructured nanomaterials of approaches have been taken to improve their gas sensing performance, for example, doping with metal or rare earth element and synthesizing received the most attention contributes to the sensing properties of the materials and much success on gas sensors. Many researchers have proved that modification of reduced Graphene oxide with SnO_2 nanoparticles is a simple method to overcome the high operating temperature problem of metal oxide gas sensors.

Moreover the optical properties of TiO_2 films, such as refractive index, extinction coefficient and scattering losses are effectively dependent on the deposition conditions. Among these techniques, DC reactive magnetron sputtering has the advantages of being capable of depositing good quality films at low substrate temperature and highly adhesion to substrate and also easy to control the deposition parameters to prepare crystalline films with relatively high reproducibility. It is evident that the improvement of materials properties requires a closer inspection of preparation conditions and also the above said properties of the films. In the present study, the author has investigated the structural, compositional, surface morphological, optical and electrical properties of TiO_2 thin films prepared by one of the solution deposition methods called chemical spray pyrolysis [1].

The sun's energy is the primary source for most energy forms found on the earth. Solar energy is clean, abundant, and renewable. Solar energy holds tremendous potential to benefit our world by diversifying our energy supply, reducing our dependence on imported fuels, improving the quality of the air we breathe, and stimulating our economy by creating jobs in the manufacture and installation of solar energy systems. Currently, a significant and growing solar industry in the world is serving customers by providing solar water heating, pool heating, and solar-electric systems [2]. However, significant benefits to consumers will only be achieved when solar energy components are successfully integrated into homes, buildings, and power plants. To date, many of the solar energy systems are significantly more expensive than the traditional options available to customers (e.g., engines, gas heaters, grid electricity).

The cost, performance, and convenience of these systems must be improved if solar energy is going to compete in energy markets against more traditional alternatives. Some large-scale solar technologies are close to being cost competitive, but the risk of making such a large investment is an obstacle to commercialization. Chiang H.Q et al, have reported that improvement of photoelectron conversion efficiency an understanding of the morphological and optical properties by reactive sputtering technique [3]. Judeinstein et al. have studied oxygen content, crystallinity and stress of TiO_2 films under the influence of the substrate temperature variation [4]. Joshi, et al. have reported the comparison of

*Corresponding author: Ayeshamariam A, Research and Development Center, Bharathiyar University, Coimbatore, 641046, India, Tel: +91 +4565-241539; E-mail: aismma786@gmail.com

the properties of TiO$_2$ films prepared by various substrates to analyse rutile and anatase phase growth direction [5]. The earlier research reported that the crystalline structure, morphology and stoichiometry of the TiO$_2$ films are responsive to the deposition conditions. Parameters such as substrate type, substrate temperature, oxygen partial pressure and deposition rate are playing an important role in the coating quality [6]. Surface structure can be divided into different ranges, shape, waviness and surface roughness that depend on the size of the surface features.

Experimental Section

TiO$_2$ doped with SnO$_2$ thin film was prepared by DC reactive magnetron sputtering technique. The precleaned glass substrates were loaded inside the vacuum chamber and Ti target (Sigma Aldrich, USA 99.99% pure) having 50 mm diameter and 5 mm thickness was used as a source. The SnO$_2$ powder (Sigma Aldrich, USA 99.7% pure) of 10% was doped with this target. The distance between the substrate and the target was maintained at 5 cm. The chamber was evacuated with rotary pump and diffusion pump better than 4×10^{-6} Torr as a base pressure. Argon was used as the sputtering gas. Oxygen was used as the reactive gas. The deposition was carried out by adjusting the various deposition parameters that is different ratios of Ar and O$_2$ substrate temperatures, sputtering power, sputtering time and distance between target and substrate, etc. X-ray diffraction (XRD) patterns of the films were recorded by PANanlytical, X'pert PRO powder diffractometer, using Cu Kα radiation (λ=1.5406 Å). The surface morphology of the films was observed by Scanning Electron Microscopy (SEM) using a digital scanning microscope HITACHI, S-3000H. For the present study, Picoscan 2000 scanning profile AFM microscopy has been used for the surface analysis of the prepared films. TEM image and selected area electron diffraction (SAED) pattern were recorded using a 200 KV Tecnai-20 G2 TEM Instrument. Electrical studies were carried out by Vander Paw method and antibacterial studies were studied for the bacteria of *Aspergillus niger* and *Aspergillus flavus*.

Results and Discussion

TiO$_2$ doped SnO$_2$ films deposited in glass substrate show the (100), (101) and (002) triplet, the characteristics of stoichiometric TiO$_2$ doped SnO$_2$ film, but the films annealed at 250°C revealed that additional plane (110) at 27.29° of rutile phase (JCPDS 21-1276) along with other peaks (101), (004), (112), (200) and (105) was observed. The SEM observations show the same trend in grain size variation as predicted by the XRD results. 90% of TiO$_2$ 10% of SnO$_2$ thin films were prepared and shows pine hole free and good adhesion on the substrate. The films prepared at room temperature shows amorphous and it becomes crystalline nature as the substrate temperature is increased up to 250°C. The peaks are identified and they are compared with the JCPDS (21-1272) data. All the peaks are assigned Miller planes and belong to anatase for the substrate temperature of 250°C. Films shows the rutile structure JCPDS (21-1276). The calculated lattice parameter values agree with the standard lattice parameter values (a=3.7852 Å and c=9.5139 Å) for tetragonal TiO$_2$ structure. The grain size is found to increase with the increase in annealing temperature. The strain and dislocation density values are found to decrease with increase in annealing temperature which results imply that the reduction in the concentration of lattice imperfections.

A layer of strongly held counter ions, in these case Ti ions adsorbed close to the charged surface on fixed sites and a diffuse layer of counter ions. This can be attributed to the process of large formation in glass substrate which releases lesser amount of TiO$_2$ doped SnO$_2$ ions in a controlled manner towards the electrode surface leading to the growth of TiO$_2$ doped SnO$_2$ film with nano grains. These results show that increasing the deposition temperature and also annealing at higher temperatures lead to highly crystalline and defect free films (Figure 1).

The average internal stress developed in the film is determined by the relation [5]:

$$S = \frac{E}{2\delta}\left(\frac{a_o - a}{a_0}\right) \tag{1}$$

where, 'E' is the Young's modulus of the film, 'δ' is the Poission's ratio of the film, 'a$_o$' is the bulk lattice constant, and 'a' is the lattice constant of the film. The film has the value of internal stress 0.02 Nm.

The origin of the strain is also related to the lattice mismatch and may be calculated from the slope of βcosθ vs. sinθ plot using the relation [5]:

$$\varepsilon = \frac{\lambda}{D\sin\theta} - \frac{\beta}{\tan\theta} \tag{2}$$

where, 'D' is the grain size, 'β' is the full width at half maximum of the peak, and 'θ' is the corresponding Bragg's peak.

$$D = \frac{0.94\lambda}{\beta \cos\theta} \tag{3}$$

The dislocation density 'δ' ie, the dislocation lines per unit area of the crystal can also be evaluated from the grain size 'D' using the formula [3,4]; crystallite size, dislocation density and number of crystallites value were tabulated in Table 1.

$$\delta = \frac{1}{D^2} \text{lines/m}^2 \tag{4}$$

Also using grain size 'D' and film thickness 't', number of crystallites 'N' has been estimated using the relation [5]:

$$N = \frac{t}{D^3} /\text{unit area} \tag{5}$$

The temperature of the substrate is a highly important process parameter influencing the film morphology. In the initial stages of the
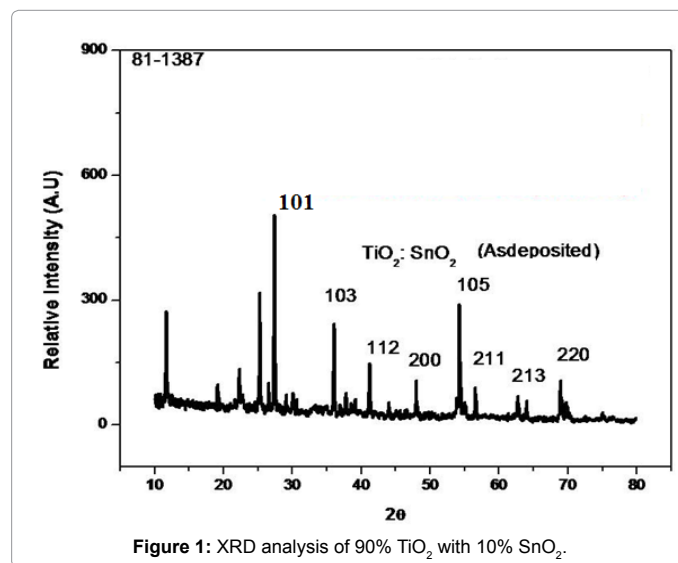

Figure 1: XRD analysis of 90% TiO$_2$ with 10% SnO$_2$.

T$_A$°C	a(Å) Calculated	c(Å) Calculated	D (nm)	δ × 10^{11} cm^{-2}	ε × 10^{-3}	Bandgap (eV)
250	3.797	9.5429	43.2	0.535	0.8373	3.866

Table 1: Structural parameters of annealed 90% TiO$_2$:10% SnO$_2$ thin films.

film growth, the flux deposited on the substrate might re-evaporate from the surface, nucleate into a cluster, be consumed by existing clusters or be trapped on a surface defect site. All these processes are dependent upon the mobility of the deposited atoms on the surface, and each has their characteristic activation energies. Such surface rearrangements are possible at higher temperatures, while at low temperature they are inhibited. Three modes of initial growth can be distinguished. Island (Volmer-Weber) [6] growth results in the formation of isolated islands on the surface. This occurs when the cohesive energy of the atoms within the film is greater than the cohesive energy between the film and atoms on the surface. Layer-by-Layer (Frank-vander Merwe) [7] growth involves a deposition of one monolayer at a time and results in a very smooth epitaxial film. It occurs when the cohesive energy between the film and the surface atoms is greater than the cohesive energy of the film atoms.

The cohesive energy will decrease monotonically as each film layer is added. Mixed growth involves growth of islands after the first monolayer has formed successfully. This occurs when the monotonic decrease in binding energy is energetically over-ridden by other factors such as strain due to lattice mismatch, with the result that island formation becomes more favorable. The substrate temperature can have a profound influence on the film growth mechanism. At low temperatures, film growth proceeds via a thermal process, enabling metastable structures to grow. At higher temperatures, grain boundaries within the film become mobile and surface diffusion and recrystallisation occurs. At the lower limit of this region, the grain boundaries of just one preferred orientation may become mobile, giving preferential growth surfaces. At higher temperatures, surface and bulk diffusion and recrystallisation occur, yielding larger crystallites. Clearly the microstructural morphology of the film is highly dependent on the growth temperature; indeed the temperature can be used as a process parameter to induce different structures [8]. Figure 2a and 2b shows the 90% TiO$_2$:10% SnO$_2$ films deposited at 200°C in which well-developed grains growing vertically are seen. At 250°C, the film shows larger grains with agglomerated particles of size about 150 nm. These observations are in support of SEM studies.

Surface morphologies of as deposited 90% TiO$_2$:10% SnO$_2$ films and the annealed films are studied by SEM and AFM analysis. Over all surface morphology is observed by SEM and a close view of the grains are studied by AFM pictures. 90% TiO$_2$:10% SnO$_2$ film deposited at 250°C shows uniform grained surface with vertically grown globular structures. The grain size is changing between about 150-250 nm. 90% TiO$_2$:10% SnO$_2$ film deposited at 250°C shows non-uniform surface. The presence of titanium and oxygen are observed in all the films as seen from (Figure 2a) for the 90% TiO$_2$:10% SnO$_2$ film deposited at 250°C respectively. EDAX shows the presence of strong titanium and oxygen signals at an approximate ratio of (Ti:O:Sn) of (1:2:0.1) for the 90% TiO$_2$:10% SnO$_2$ films deposited at 250°C deposited film. The EDX spectrum for the 250°C air annealed film is shown in Figure 2b, there is no impurities are in the EDX spectra. The atomic percentage for Ti:O:Sn is found to be about 30.11:60.04:9.85 which equal to 1:2:0.1 ratio.

AFM results of 90% TiO$_2$:10% SnO$_2$ films at 250°C of 2D and 3D with roughness graph are shown in Figure 3a and 3b respectively, from which well crystallized and grown grains are observed. They reveal a compact polycrystalline film. The morphology is granular with almost uniform size distribution of grains. Root mean square roughness is the oftenly used amplitude parameter equal to the surface heights relative to the least square fitted line of the profile. Expressed as an equation, it is defined as [9]
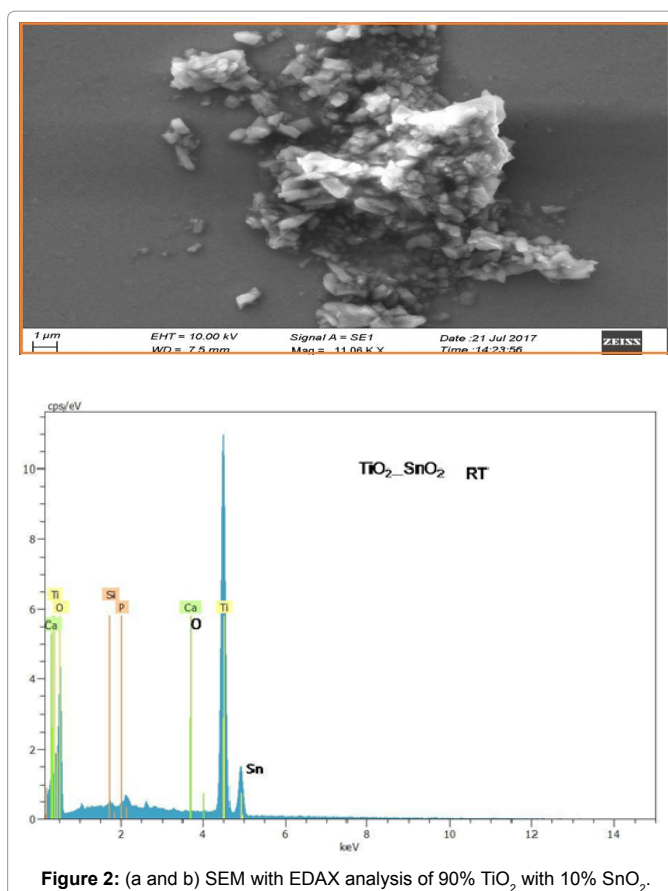

Figure 2: (a and b) SEM with EDAX analysis of 90% TiO$_2$ with 10% SnO$_2$.

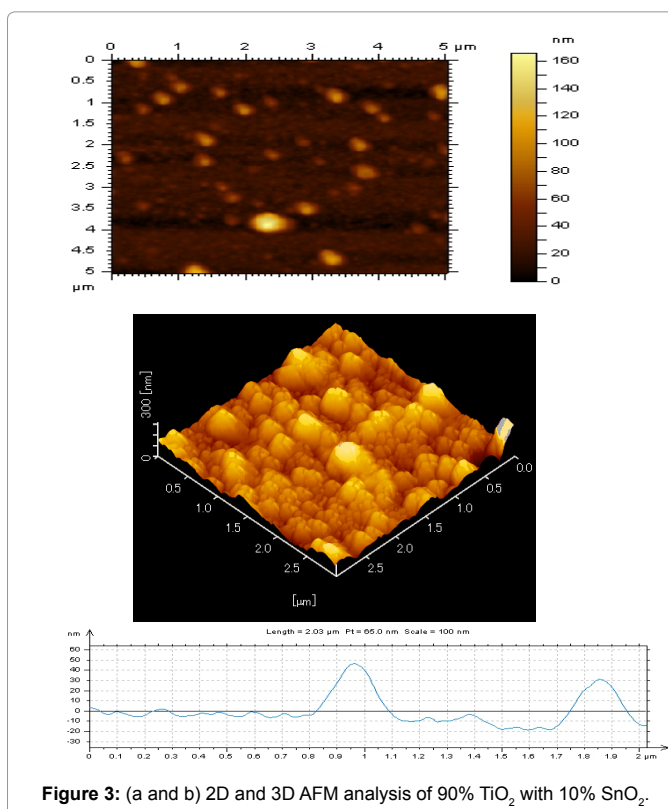**Figure 3:** (a and b) 2D and 3D AFM analysis of 90% TiO$_2$ with 10% SnO$_2$.

$$\text{rms roughness} = \sqrt{\left[\frac{1}{L}\int_0^L z^2(x)\right]dx} \qquad (6)$$

$$= \sqrt{\left[\frac{1}{N_L}\sum_L Z_i^2(x)\right]} \qquad (7)$$

where, 'L' is the cutoff length, 'N_L' is the number of discrete measurement point and '$Z_i(x)$' is the height deviation of the profile from a least square fitted line that eliminates the slope or shape of the entire profile. The roughness value of this film is equal to 14 ohm-sq-m. The evolution of the optical property can be explained by the phase transformation and the growth of particle size. Figure 4a-4c shows the absorption spectra
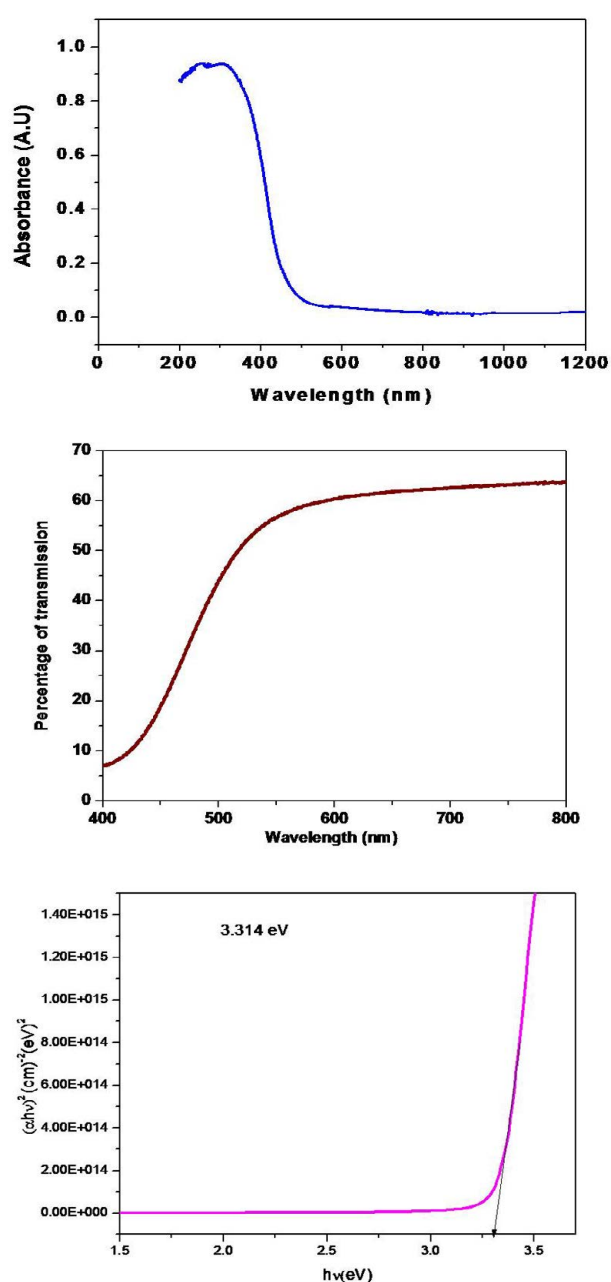

Figure 4: (a-c) Absorbance, transmittance and bandgap values of 90% TiO$_2$ with 10% SnO$_2$.

of 90% TiO$_2$:10% SnO$_2$ films as-deposited and annealed at 250°C. It is seen that with increasing annealing temperature the absorption edge shifts to the lower wavelength direction. This result proves that the absorption edge of 90% TiO$_2$:10% SnO$_2$ film moves to visible spectrum range, which indicates that the TiO$_2$ films is sensitive to visible light. Figure 5a and 5b shows the typical TEM image of the deposited 90% TiO$_2$:10% SnO$_2$ film. Densely packed nano crystals with a diameter of 25-30 nm are observed. Selected area electron diffraction pattern (SAED) was recorded and shown in (Figure 5b).

The SAED pattern shows diffused as well as, well defined rings, indicating the TiO$_2$ film is polycrystalline consists of nanoparticles. Single phase anatase formation is confirmed from the calculated d-spacing of the rings corresponding to (101), (103), (200) and (105) lattice planes. The deposited film shows uniform and closely packed nano grains of size 25-40 nm. According to the SAED diffraction rings, the films are assumed to have nano crystallites as well as polycrystalline nature. The lattice spacing values calculated from the strong diffraction circles are 3.540 Å, 2.382 Å and 1.703 Å which coincide with those of anatase phase. The assigned (101), (004), (105) planes confirm the formation of nano grained 90% TiO$_2$:10% SnO$_2$ film deposited [10].

The optical bandgap E$_g$ can be determined from absorption spectrum as well as the transmittance spectra. The absorption coefficient α depends on the wavelength λ are shown in Figure 4a. The films are highly transparent in the visible region as in the case of 90% TiO$_2$:10% SnO$_2$ films. These spectra were recorded in the transmission configuration with glass substrate as reference in the UV-Vis-NIR spectrometer. The films are highly transparent in the visible region as in the case of 90% TiO$_2$:10% SnO$_2$ films.

Figure 4b shows the transmittance spectra of as deposited and annealed 90%TiO$_2$:10% SnO$_2$ films. The films annealed at 250°C shows a significant increase with a steeper optical transmission curve which is about 70% transmittance in the visible region. It indicated lower defect density near the band edge. The increase in optical transmittance with rise of annealing temperature can be attributed to the increase of structural homogeneity and the decrease of defect. Figure 4c band gaps of the films are evaluated from the sharply falling transmission region. Tauc method [11] is employed in the high absorbance region of the transmittance spectra. From the Table 1, it is observed that the indirect optical band gap value increases when annealing temperature increases. This increase may be attributed to the enhancement of crystallinity nature. Whereas the direct optical band gap values slightly changes, it may be changed in the shape of the fundamental absorbance edge. For direct transitions in Figure 4c the intercepts of the two straight lines occur at 3.37 eV [12]. FT-IR spectra of the 90% TiO$_2$:10% SnO$_2$ films, presence of characteristic peaks confirm that the deposited films are of good quality. Appearance of bands in the FT-IR spectrum is only
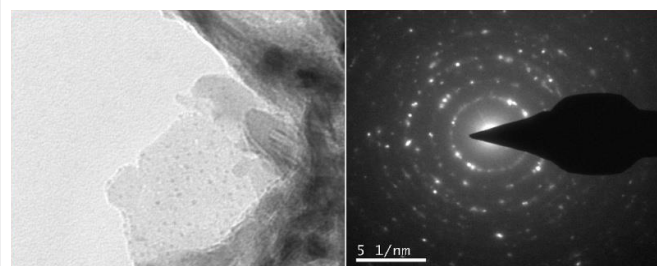
Figure 5: (a and b) TEM with SAED pattern analysis of 90% TiO$_2$ with 10% SnO$_2$.
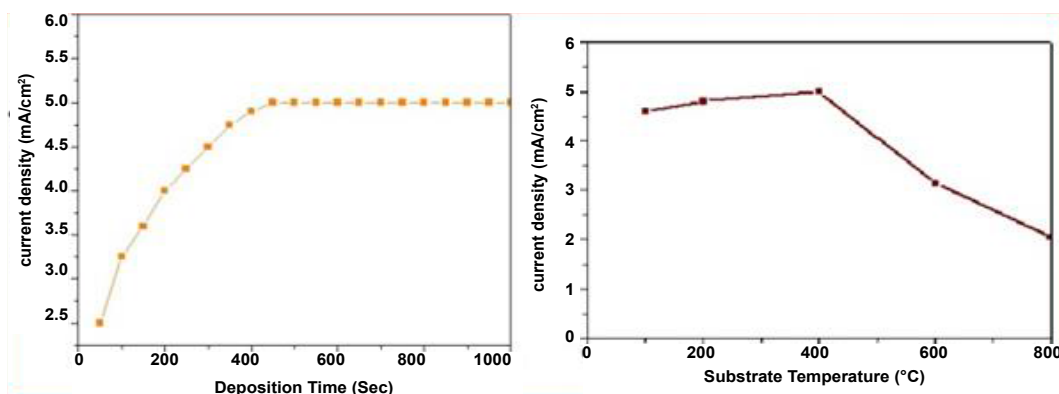
Figure 6: (a and b) Variation of current density with deposition time (Sec) and Variation of current density with substrate temperature (°C).

ascribed to TiO$_2$ nanoparticles. Peaks located at 461, 469, and 465 cm^{-1} are closely assigned to stretching vibration of Ti-O band in the TiO$_2$ lattice respectively [13]. No other phases or impurities are observed shown in Figure 6a. 90% TiO$_2$ and 10% SnO$_2$ thinfilm is an n-type semiconductor due to donor-like oxygen vacancies, so that the electrical conductivity of 90% TiO$_2$ and 10% SnO$_2$ thinfilm is proportional to the concentration of oxygen vacancies, which in turn depends on the ambient oxygen pressure [14].

Figure 6b shows the variation of current density mA/cm^2 with deposition time for the 90% TiO$_2$ and 10% SnO$_2$ thinfilm deposited at 200°C. Figure 6a and 6b shows the variation of current density mA/cm^2 with substrate temperatures of 90% TiO$_2$ and 10% SnO$_2$ thinfilm at 250°C. The conduction mechanism of the 90% TiO$_2$ and 10% SnO$_2$ thinfilm is related to the vacancies existing in the structure. The electrical properties of 90% TiO$_2$ and 10% SnO$_2$ thinfilm is associated with their microstructure and composition and consequently on the deposition parameters. In this study, the 90% TiO$_2$ and 10% SnO$_2$ thinfilm was oriented in both R (110) and A (101) directions. The resistivity values obtained is about 2.0 to 8.0 × 10^3 Ωcm in this work may be due to the fact that substrate temperature of the films brought about non-stoichiometric 90% TiO$_2$ and 10% SnO$_2$ thinfilm. It is clearly evident that the increase of temperature is associated with a reduction in film resistivity. This can be described by the increased number of thermally excited electrons in the TiO$_2$ film [15]. There slopes are observed in the curve, which can be fit with the relation proposed [16].

$$\rho = \rho_o \exp(\Delta E/kT) \tag{8}$$

where ρ_o is a constant, k is the Boltzmann constant and T is the absolute temperature and ΔE is the activation energy. Three activation energies are inferred, ΔE=0.61 eV, 0.24 eV and 0.08 eV, which are in good agreement with the reported activation energy values [17] by eqn. (8). The change in resistivity is due to either the variation in the electron mobility and the mean free path of electrons and their concentration. The carrier concentration measured for this film is in the range of 10^{19}-10^{20} cm^{-3}.

Conclusion

The microstructure, optical and electrical properties of the TiO$_2$ doped with SnO$_2$ thin films of anatase phase were confirmed by XRD and EDAX analysis. The activation energy calculated from the resistivity versus temperature variation has been found to be E$_a$=0.69 eV for the film deposited at 250°C. EDX confirmed the presence of Ti, Sn and O. Surface morphology by SEM and AFM shows uniform and pin hole free films. Uniform surface coverage with fine-grained structure was observed from SEM, TEM and AFM analysis. FTIR and TEM results confirmed the formation of monophase TiO$_2$ doped with SnO$_2$ films with nano grains.

References

1. Kim HC, Gilmore M, Pique A, Horwitz JS, Mattoussi H, et al. (1999) Electrical, optical, and structural properties of indium-tin-oxide thin films for organic light-emitting devices. Journal of Applied Physics 86: 6451-6461.

2. Isaac J, Ordejón P, Canto G, Mozos JL, Fraxedas J, et al. (2002) Designed Self-Doped Titanium Oxide Thin Films for Efficient Visible-Light Photocatalysis Advanced Materials 14: 1399-1402.

3. Chiang HQ, Wager JF, Hoffman RL, Jeong J, Keszler AD (2005) High mobility transparent thin-film transistors with amorphous zinc tin oxide channel layer. Applied Physics Letters 86: 013503.

4. Judeinstein, Patrick, Livage J (1991) Sol–gel synthesis of WO3 thin films Journal of Materials Chemistry 1: 621-627.

5. Joshi RN, Singh VP, McClure JC (1995) Characteristics of Indium Tin Oxide Films Deposited by R.F. Magnetron Sputtering. Thin Solid Films 257: 32-35.

6. Asahi RY, Morikawa OJI, Ohwaki T, Aoki TK, Taga Y (2001) Visible-light photocatalysis in nitrogen-doped titanium oxides. Science 293: 269-271.

7. Davide B (2001) Composition and Microstructure of Cobalt Oxide Thin Films Obtained from a Novel Cobalt(II) Precursor by Chemical Vapor Deposition. Chemistry of Materials 13: 588-593.

8. Nie X, Leyland A, Matthews A (2000) Deposition of layered bioceramic hydroxyapatite/TiO2 coatings on titanium alloys using a hybrid technique of micro-arc oxidation and electrophoresis. Surface and Coatings Technology125: 407-414.

9. Minami T (2008) Present status of transparent conducting oxide thin-film development for Indium-Tin-Oxide (ITO) substitutes Thin Solid Films 516: 5822-5828.

10. Ahmed T, Rack HJ (1998) Phase transformations during cooling in α+β titanium alloys. Materials Science and Engineering: A 243: 206-211.

11. Tauc JJ (1974) Amorphous and Liquid Semiconductors, Plenum, London.

12. Viezbicke Brian D (2015) Evaluation of the Tauc method for optical absorption edge determination: ZnO thin films as a model system. physica status solidi (b) 252: 1700-1710.

13. Zhang, Jun-Ying, Boyd IW (1996) Efficient excimer ultraviolet sources from a dielectric barrier discharge in rare-gas/halogen mixtures. Journal of Applied Physics 80: 633-638.

14. Kavith RS, Meghani Jayaram V (2007) Materials Science and Engineering 139: 134-140.

15. Stamate, Marius D (2000) Preparation of oriented poly (vinylidene fluoride) thin films by a cost-effective electrostatic spray-assisted vapour deposition-based method. Thin Solid Films 372: 246-249.

16. Akl AA, Kamal H, Abdel-Hady K (2006) Fabrication and characterization of sputtered titanium dioxide filmsApplied surface science 252: 8651-8656.

17. Shinde SR (2004) Co-occurrence of superparamagnetism and anomalous Hall effect in highly reduced cobalt-doped rutile TiO2−δ films. Physical Review Letters 92: 16660.